Journal of Environment, 1, (2014), 28–35:

Original Paper

Predicting Flood Vulnerable Areas by Using Satellite Remote Sensing Images in Kumamoto City - Japan

A. Besse Rimba [a,]*, Fusanori Miura [b]

[a] *Center for Remote Sensing and Ocean Science (CReSOS), Udayana University, PB Sudirman street, Denpasar, Bali, 80232 Indonesia*

[b] *Graduate School of Science and Engineering, Department of Environmental Science and Engineering, Yamaguchi University, 2-16-1 Tokiwadai, Ube 755-8611, Japan*

* Corresponding author: Andi Besse Rimba; E-Mail: a.besserimba@yahoo.com
Tel./Fax.: +62 361 256 162

Received: 18 February 2014 / Accepted: 26 September 2014 / Published: 03 October 2014

***Abstract*:** Flood is a natural disaster that occurs almost every year in Japan. Based on the flood record, it occurs during the rainy season around July each year. The aim of this research is to predict areas vulnerable to flood. The current research location is the Shiragawa watershed. This study was carried out using DEMs data, ALOS AVNIR-2 and Amedas data to produce watershed area, vegetation index, land cover map and isohyet map. DEM data with spatial resolution of 10 meters was derived from the Geospatial Information Authority of Japan (GSI) in order to show the watershed. The AVNIR-2 imagery was used to create the land cover map and the vegetation index. The land cover map was created by unsupervised method then verified by using land cover map of the Geospatial Information Authority of Japan (GSI). Vegetation index was created by using Normalize Vegetation Index (NDVI) algorithm. The isohyet was obtained using data from rain gauges stationed in Kumamoto Prefecture then interpolating by applying the kriging method. All spatial data was overlaid to create the flood vulnerability map by using Geographic Information System (GIS). This study combines all the data to predict vulnerable areas of flood. The result indicates that the flood occurs in the middle part of Shiragawa watershed.

***Keywords*:** Flood; satellite imagery; GSI; GIS; Shiragawa watershed

---

1. Introduction

Flood is a natural phenomenon. Flood occurred is not only caused by rainfall but also by many such as ice jam/clogging, collapse of dikes or other protective structures, storm surge, tsunami, high tide, cloud burst, lake outburst, slope instability in watershed and debris flow (Eximap, 2007)

In 2012, a flood occurred in Kumamoto Prefecture in Kyusu Island. The flood in Kumamoto Prefecture was caused by heavy rain in Mt. Aso. The flat area in Kumamoto City became inundation area. The high rainfall intensity resulted in rapid flooding and earth slides. The largest affected area by the flood in 2012 is the Shiragawa river. Floods occur when large volumes of runoff flow quickly into streams and rivers. The peak discharge of a flood is influenced by many factors, including the intensity and duration of storms and snowmelt, the topography and geology of stream basins, vegetation, and the hydrologic conditions preceding storm and snowmelt events (Konrad, 2000).

The satellite imagery can predict and detect the flooded area. This research used the ALOS data to estimate the flood vulnerability area. By applying DEMs, it can conduct topography analysis and inundation areas. This will contribute to advance methods for analyzing and investigating those phenomena. At the same time, vegetation index, rainfall distribution and land cover data will improve the reliability of these analyses as well as flood vulnerability area. The high resolution of DEMs image gives detail information about the topography. Vegetation index and land cover give information about the vegetation density and the land surface cover. The rainfall data show the distribution of precipitation which involved the flood vulnerability area.

Combining some parameters can be done by using The Geographic Information System (GIS). Each feature in GIS has score. By applying the scoring method, the flood vulnerability area can be predicted. All parameters are overlaid to determine the flood vulnerability area.

2. Research Methodology

The research location is Shirakawa watershed in Kumamoto Prefecture. This area always flooded every heavy rainy season. The research boundary can be seen in Figure 1.

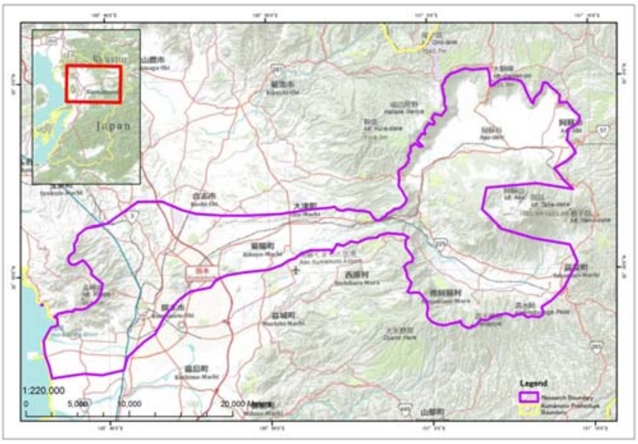

Figure 1. Research area boundary

2.1. Data collection

The data used in this research is secondary data. It derived from the satellite imagery and government/organization data. The remote sensing data is the main data for this research. Remote sensing data is very important in this research. Some substantial data are derived from ALOS AVNIR-2 imagery such as vegetation index and land cover classification. This research used DEM data from GSIDEM data with 10 mesh and 5 mesh. The spatial resolution of 10 mesh is 0.4 second (10 meters) and 5 mesh is 0.2 second (5 meter). DEM derived to get slope data and river pattern. From river pattern, watershed can be created. Rainfall data used in this research are rainfall averages in rainy season (July 2012) in Kumamoto Prefecture. The aim of using the GSI Map and Google Earth in this research is verification the parameters of this research. In this case, the land cover and the NDVI are verified with these data.

2.2. Data analysis method

Analyzing satellite data were started by pre-processing ALOS AVNIR-2 which the radiometric and geometric correction. In this research used vegetation index algorithm and land cover classification, A normalized Different Vegetation Index (NDVI) was used to determine the vegetation index. Green leaves have a reflectance of 20% or less in the 0.5 to 0.7 micron range (green to red) and about 60% in the 0.7 to 1.3 micron range (near-infrared). These spectral reflectance are themselves ratios of the reflected over the incoming radiation in each spectral band individually; hence, they take on values between 0.0 and 1.0. Thus, the NDVI itself varies between -1.0 and +1.0.

The NDVI process creates a single-band dataset that mainly represents greenery. The negative values represent clouds, water, and snow, and values near zero represent rock and bare soil. The documented and default NDVI equation is as follows:

$$NDVI = ((IR - R)/(IR + R)) \tag{1}$$

Where :

IR = pixel values from the infrared band

R = pixel values from the red band

This index outputs values between -1.0 and 1.0. Very low values (0.1 and below) of NDVI correspond to barren areas of rock, sand, or snow. Moderate values (0.2 to 0.3) represent shrub and grassland, while high values (0.6 to 0.8) indicate temperate and tropical rainforests.

Land use cover (LUC) assessment is one of the most important parameters to meaningfully plan for land resources management. LUC inventories are assuming increasing importance in various resources sectors like agricultural planning, settlements surveys, environmental studies and operational planning based on agro-climatic zones. The knowledge of spatial land cover information is essential for proper management, planning and monitoring of natural resources (Zhu, 1997). Satellite remote sensing imagery is a viable source of gathering quality land cover information at local, regional and global scales (Csaplovics, 1998; Foody, 2002). It can be seen in Table 1.

A digital elevation model (DEM) consists of terrain elevations for ground positions at regularly spaced horizontal intervals. DEMs can be used, for example, in the generation of three-dimensional graphics displaying terrain slope, aspect, and terrain profiles between selected points. DEMs have become an important source of topographical data for many scientific and engineering uses, such as hydrological and geological studies, infrastructure planning and environmental applications. Where topographical data is unavailable, global coverage elevation data sets, typically DEMs from remotely sensed data can be the main source of information. DEM generation techniques and DEM quality assessment includes applications in difficult environments, such as pre- or post-earthquake events and volcanoes (e.g., d'Ozouville et al., 2008; Hirano et al., 2003; Wang et al., 2007).

Table 1. Land use/land cover classification scheme by The land use cover types were stratified according to the U.S. Geological Survey's land-Use/Land-cover classification system for Use with Remote Sensor Data (Anderson et al., 1976).

Item	Description
Build-up land	Area that have been populated with residential, commercial, industrial, transportation and facilities.
Forest of rangeland	Area covered with mature trees, shrubby plants and other plants growing close together.
Water	Area covered with water such as river and lakes
Agricultural land	Rain fed cropping, planted and irrigated cropping areas, areas covered mainly with herbaceous vegetation with shrubs
Barren land	Mountainous or hill areas, areas with no vegetation cover, degraded land and all unused area.

Isohyet is a line drawn on a weather map connecting points that receive equal amounts of precipitation during a given period of time. An isohyet map is a map that displays precipitation data. The contoured lines connect areas of equal rainfall, and many times a color scale is used to differentiate between areas. Isohyet maps are prepared by interpolating rainfall data recorded at gauged points. (Ven Te Chow, 1964). The flood parameters were

Table 2. Watershed characteristic as flood/run-off parameters (Ven T. Chow, with modification)

Parameters	Units	Category	Score	Data source	Description
Slope **(1st parameter)**	30%	steep	20	Topography map DEM	Topography map GSIdem
	10 – 30%	mountainous	15		
	5 – 10%	surge	10		
	0 – 5%	relatively flat	5		
Vegetation cover **(2nd parameter)**	Vegetation high density	low	5	Satellite interpretation	Satellite imagery
	Vegetation medium density	moderate	10		
	Vegetation low density	high	15		
	Settlement hardened surface	high	20		
Rainfall **(3rd parameter)**	<20 mm/ 24 hours	low	5	• AMEDAS	• satellite imagery
	21-50 mm/hours	moderate	10		
	51-100 mm/hours	high	15		
	>100 mm/hours	extreme	20		

combined to determine the vulnerability area. It can be seen in Table 2.

Figure 1 shows the flow chart that explained about the proses of this research. In this research, there is 3 data sources that was used in this research: DEM, ALOS AVNIR-2 and Rainfall.

3. Results and Discussion

3.1. Shiragawa watershed map

Watershed map was derived from DEM data. The spatial resolution is 10 meters which equal to 0.4 second or 10 mesh. It was converted to raster by using point to raster tool in ArcGIS 10 to determine DEM data. It was delineated base on the valley and ridge around the Shiragawa river. The area of Shiragawa watershed is Aso City, Minamiaso Mura, Ozu Machi, Kikuyo Machi, Koshi City and Kumamoto City. Base on the map as shown in Figure 1, the total area of Shirakawa watershed is 559.678606 km^2.

3.2. Slope map

The slope map was derived from GSIDEM data by using ArcGIS 10. It has convert from slope in percent to slope in degree. The slope of Shiragawa watershed is unique that in Minamiaso Mura is hilly steep and mountainous area. Aso City, Kikuyo, Koshi City and Kumamoto City are relatively flat. Some areas in east part of Kumamoto City are surge. Base on the slope map, the Shiragawa watershed area is mostly relative flat and mountainous area. In the Aso City where is this area located in Mt. Aso has unique pattern also, this area should be mountainous area but this area is relatively flat. This area is accumulation area of pyroclastic which causes area of Shiragawa watershed is rich by alluvial material. The area of slope in Shirakawa watershed can be seen in Table 3. It shows the area each degree of slope. Area with slope 0 - 5 % has a lot distribution in Shirakawa watershed.

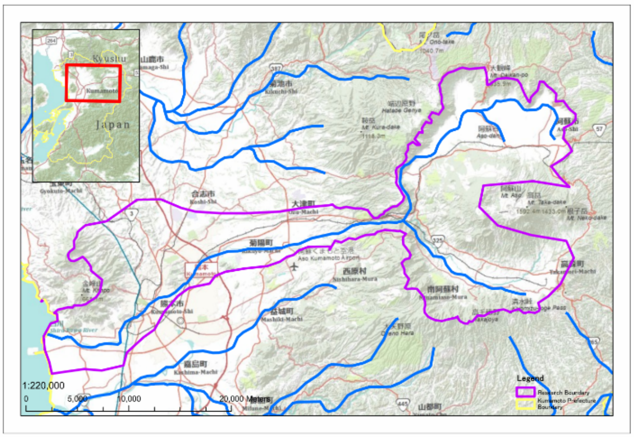

Figure 2. The Shiragawa watershed and research boundary map

Table 3. Total Area of slope in Shirakawa watershed

slope	Area (m^2)	Area (km^2)
>30 %	388138	0.388138
10 – 30 %	55732112	55.732112
5 – 10 %	91914136	91.914136
0 – 5 %	411644220	411.64422
Total	559678606	559.678606

Figure 3 shows that in the west side of Shirakawa watershed is a mountainous area whereas is Mt. Aso area. It is the upper area. In the middle of Shirakawa watershed is flat area then in the east part is surge and relatively flat. This pattern makes the middle part of Shirakawa watershed is like hollow. The hollow area becomes a pool area when the rainfall season.

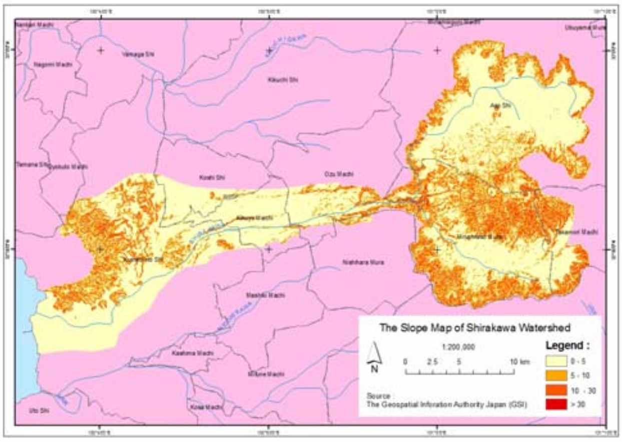

Figure 3. Slope map

3.3. Vegetation Index

The Normalized Vegetation Index was derived from ALOS AVNIR-2 by Equation 1. The Normalized Vegetation Index was used in this study for determining the land cover area. The Land cover and the NDVI were collaborated to determine flood vulnerability parameter. The result shows that the area of Shiragawa watershed has high vegetation density in Minamiaso Mura. This is upper area. It has range value between 0.3-0.58. It indicated that this area is the highest vegetation density. In the middle area of Shiragawa watershed has low value, it indicated this area has low vegetation or hardness surface. The distribution of vegetation index can be seen in Figure 4. Table 4 shows the total area of vegetation each categories of vegetation index.

3.4. Land cover map

The Land cover map was derived from ALOS AVNIR-2. The IsoData unsupervised classification was applied to determine this map. This map was verified by using the google map and the landcover of the Geospatial Information Authority of Japan (GSI). It was classified into 6 classes: cloud, water bodies, mixing farm, forest or high vegetation, hard surface and bare land. The ALOS AVNIR-2 which was determined the land cover that was covered by cloud. The cloud covers the information on the ground. In this research, the cloud was not erased and replaced by other data. The distribution of land cover can be seen in Figure 5. The area of land cover for the Shirakawa watershed can be seen in Table 5.

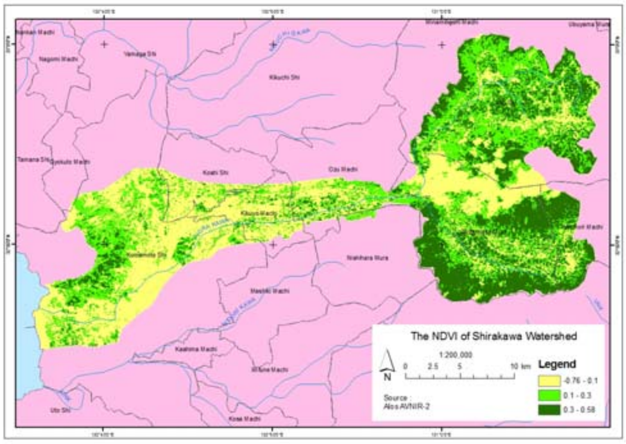

Figure 4. Vegetation Index

Table 4. Total Area of vegetation index in Shirakawa watershed

Vegetation Index	Area(m^2)	Area (km^2)
(-0.75-0.1)	213397776	213.398
(0.1-0.3)	110917970	110.918
(0.3-0.58)	235362860	235.363
Total	559678606	559.679

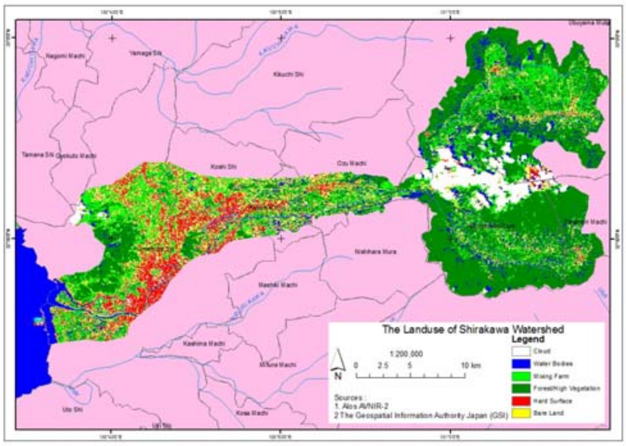

Figure 5. Land cover map

Table 5. Total area of land cover in Shirakawa watershed

land cover	Area (m^2)	Area (km^2)
forest	235362860	235.36286
hard surface	50240836	50.240836
bare land	80557840	80.55784
mixing farm	110917970	110.91797
water body	42492680	42.49268
cloud	40106420	40.10642
Total	559678606	559.678606

3.5. Rainfall map

The result shows that the highest rainfall distribution in July 2012 is in Mt. Aso at Aso City. This is the upper of Shiragawa watershed. The material of this area is pyroclastic from Mt. Aso which contain with alluvial. If the high rainfall occurs in upper of Shiragawa watershed, the middle or the low part of Shiragawa watershed will be affected. The rainfall of middle and low part of Shiragawa watershed are 20 – 30 mm/day. This is not a big value for causing the flood if the upper part of watershed has small rainfall value also. Base on this map, the dominant value is 20 – 30 mm/day. It should be not affected flood, if there is no other parameter which can be affected the flood. The distribution of rainfall can be seen in Figure 6. The total area of rainfall can be seen in Table 6.

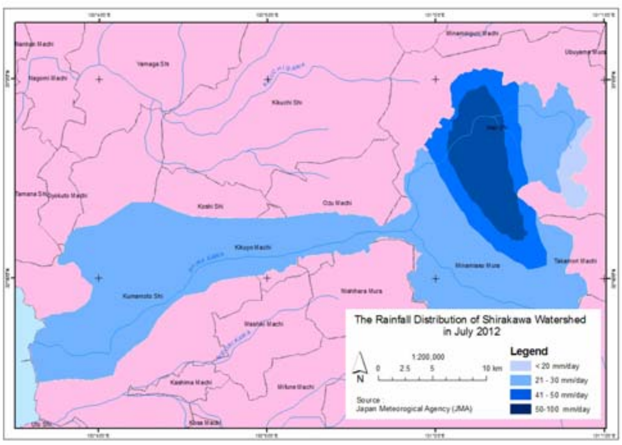

Figure 6. Rainfall map

Table 6. Total area of rainfall distribution in Shirakawa watershed

rain	m^2	km^2
<20 mm/day	13900684	13.900684
21 – 30 mm/day	487602050	487.60205
41 – 50 mm/day	58175872	58.175872
Total	559678606	559.678606

3.6. Flood vulnerability map

The Flood Vulnerability Map is a final map for this research. It was created by combining 3 parameters which is the slope map, land cover map and rainfall map. This is using the weighting method for determining the class value. Each feature on the maps has a value. This value was determined by using Ven T. Chow with modification. Each parameter has equal weight. The level of vulnerability was categorized into 5 classes. The levels are very low, low, medium, high and very high. The classes was determine by using equal interval method where is the maximum range value subtracted by the minimum range value then divided with number of class. In this case, the number of class is 5 classes. The maximum value is 60 and the minimum value is 15. In this research, the interval class value is 8. By using this method and the pattern of parameters, the highest vulnerable area is in middle of Shiragawa watershed. The cloud still covered the information its below because this research used image data only as primary data. The total area of flood vulnerable area can be seen in Table 7. The distribution off flood vulnerable areas can be seen in Figure 7.

The vulnerability map shows that the low area has high flood vulnerability. It was caused by settlement area so that the rainfall became runoff surface and less vegetation density. In the upper of shiragawa watershed has low flood vulnerability, it was caused that this area has high vegetation density and the it was covered by forest. In other hand, this area has steep and mountainous slope. The slope failure can occur in this area.

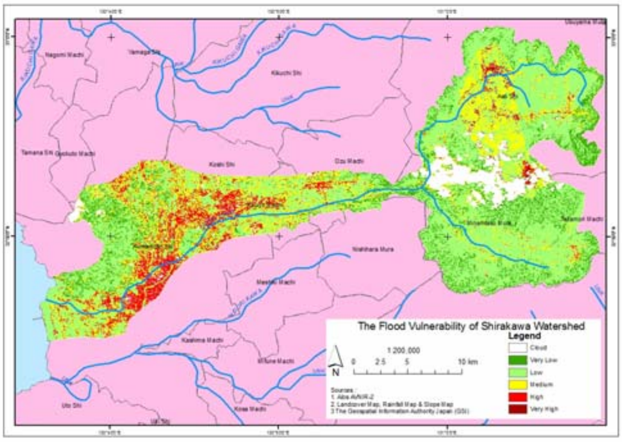

Figure 7. Flood vulnerability

Table 7. Total area of flood vulnerability in Shirakawa watershed

vulnerability	m^2	km^2
Very Low	17465699	17.4657
Low	242119156	242.1192
Medium	184561400	184.5614
High	114324860	114.3249
Very High	1207491	1.207491
Total	559678606	559.6786

The upper part of Shirakawa watershed has high vegetation density and slope is steep and mountainous, it caused that area did not become the flooded area. In the upper part of watershed, the flood did not occur because the slope is step and mountainous but other disaster can be occurs such as land slide.

For determining the flood vulnerability area should be use some parameters. In this case, vegetation covered should be protected this watershed. But in the fact, this area is always flooded. Mostly area is flat and covered by vegetation. But this area has high flood vulnerability in rainy season, maybe it is caused by other parameters such as soil. The most vulnerable area is about 115.59 km2 from total area 559 km2.

For determining the flood vulnerability area, there are many methods that can be used. This research is only one way to produce the vulnerability map. The vulnerability area on this paper was produced base on the satellite image only. This result is needed to be verified by field survey and historical flood data.

4. Conclusions

This research produced the flood vulnerability area by using the ALOS AVNIR-2, DEMs and the rainfall data from AMEDAS data. There some method can be used to determine the flood vulnerability area. Base on this research, the vulnerability area located in Kumamoto City. It was caused because this area has high score in land cover parameter, high score in slope parameter and middle sore in rainfall parameter. This area covered by hardened surface and has relatively flat slope. The high rainfall in the upper part of Shiragawa watershed caused flooding in the middle part of watershed.

In the upper part of Shiragawa watershed, the flood did not occur because this area has low score of slope and land cover. The topography in this area is mountainous and the land cover is forest which has high vegetation index. Even though this area has high rainfall distribution but other parameters were not suitable for affecting flood. The flood may not occur but other natural disaster such as land slide can occur.

Acknowledgments

This work was supported by CReSOS and JAXA mini-ocean projects in Indonesia. We thank DIKNAS (ministry of education of Indonesia) for financial support.

References

Arcgis. 2013. NDVI function. May 25, 2013. Available from: URL: http://resources.arcgis.com/en/help/main/10.1/index.html#/NDVI_function/009t00000052000000/

Chander, G., B. L. Markham and D. L. Helder. 2009. Summary of Current Radiometric Calibration Coefficients for Landsat MSS, TM, ETM+, and

EO-1 ALI sensors. Remote Sensing of Environment. 113 : 893-903.

Chow, Ven Te, Maidment David R. and Mays Larry W. 1964. Applied Hydrology. California : McGraw-Hill International Edition Civil Engineering Series. June 18,2013. Available from:URL :http://www.scribd.com/doc/29283580/Applied-Hydrology-by-Ven-Te-Chow-David-R-maidment-Larry-W

Csaplovics, E. 1998. High Resolution Space Imagery for Regional Environmental Monitoring — Status Quo and Future Trends. International Archives of Photogrammetry and Remote Sensing. 32(7) : 211-216.

D'Ozouville, N., Deffontaines, B. Benveniste, J. Wegmuller, Violette and De Marsily. 2008. DEM Generation Using ASAR (ENVISAT) for Addressing The Lack of Freshwater Ecosystems Management, Santa Cruz Island, Galapagos. Remote Sensing of Environment. 112(11) : 4131-4147.

EXCIMAP (European Exchange Circle on Flood Mapping). 2007. Handbook on good : practices for flood mapping in Europe. France : Eximap Press Inc.

Japan Aerospace Exploration Agency. 2008. ALOS Data Users Handbook Revision C. April 17, 2013. Available from: URL: http://www.eorc.jaxa.jp/ALOS/en/doc/fdata/ALOS_HB_RevC_EN.pdf

Konrad, C.P. 2000. Effects of Urban Development on Floods. U.S. Geological Survey Water- Fact Sheet 076-03. June 07,2013. Available from: URL: http://pubs.usgs.gov/fs/fs07603/.

Lillesand, T., R. Kiefer, J. Chipman. 2007. Remote Sensing and Image Interpretation. 6th Ed. United State of America : John Wiley & Sons. Inc.

Otto, Huisman and A. Rolf . 2009. An Introductory Textbook - Principles of Information Systems. Enchede, Netherland : ITC.

Singh, V.P., and P.K. Chowdhury. 1986. Comparing Methods of Estimating Mean Areal Rainfall. Water Resource Bulettin. 22 (2) : 275-282.

Zhu, A X. 1997. Measuring Uncertainty in Class Assignment for Natural Resource Maps Under Fuzzy Logic. Photogrammetric Engineering and Remote Sensing. 63 (10) : 1195-1202.